



HAL
open science

Diffusion of homologous model migrants in rubbery polystyrene: molar mass dependence and activation energy of diffusion

Jérémy Pinte, Catherine Joly, Patrice Dole, Alexandre Feigenbaum

► To cite this version:

Jérémy Pinte, Catherine Joly, Patrice Dole, Alexandre Feigenbaum. Diffusion of homologous model migrants in rubbery polystyrene: molar mass dependence and activation energy of diffusion. Food additives & contaminants. Part A. Chemistry, analysis, control, exposure & risk assessment, 2010, 27 (04), pp.557-566. 10.1080/19440040903441461 . hal-00576971

HAL Id: hal-00576971

<https://hal.science/hal-00576971>

Submitted on 16 Mar 2011

HAL is a multi-disciplinary open access archive for the deposit and dissemination of scientific research documents, whether they are published or not. The documents may come from teaching and research institutions in France or abroad, or from public or private research centers.

L'archive ouverte pluridisciplinaire **HAL**, est destinée au dépôt et à la diffusion de documents scientifiques de niveau recherche, publiés ou non, émanant des établissements d'enseignement et de recherche français ou étrangers, des laboratoires publics ou privés.



DIFFUSION OF HOMOLOGOUS MODEL MIGRANTS IN RUBBERY POLYSTYRENES: MOLAR MASS DEPENDENCE AND ACTIVATION ENERGY OF DIFFUSION

Journal:	<i>Food Additives and Contaminants</i>
Manuscript ID:	TFAC-2009-143.R1
Manuscript Type:	Original Research Paper
Date Submitted by the Author:	21-Oct-2009
Complete List of Authors:	Joly, Catherine; UMR INRA URCA FARE; ESIEC Joly, Catherine; University of Lyon 1, LRGIA- IUT
Methods/Techniques:	Chromatographic analysis
Additives/Contaminants:	Packaging overall migration, Packaging plasticisers, Plasticisers, Simulants
Food Types:	

SCHOLARONE™
Manuscripts

1
2
3
4
5
6
7 **1 DIFFUSION OF HOMOLOGOUS MODEL MIGRANTS IN RUBBERY POLYSTYRENE:**
8 **2 MOLAR MASS DEPENDENCE AND ACTIVATION ENERGY OF DIFFUSION**
9

10
11 3
12 4
13 5 Jérémy Pinte^a, Catherine Joly,^{a,b*} Patrice Dole^a, Alexandre Feigenbaum^a
14
15

^a	UMR FARE (INRA-URCA), Moulin de la Housse, BP 1039, 51867 Reims Cedex 2, France
^b	ESIEC (Ecole Supérieure d'Ingénieurs en Emballage et Conditionnement), Pôle Technologique Henri Farman, BP 1029, F-51686 Reims Cedex 2, France
*	Corresponding author. (Phone: +33 326 91 38 22, fax:+33 326 91 39 16)

16
17
18
19
20
21
22
23 6
24 7
25 8
26 9 **ABSTRACT:**
27

28
29
30
31
32
33
34
35
36
37
38
39
40
41
42
43
44
45
46
47
48
49
50
51
52
53
54
55
56
57
58
59
60

10 The published diffusion prediction models devoted to the diffusion of additives in food
11 packaging simplify reality by having only a few parameters. Therefore, extrapolation of such
12 models to barrier polymers, larger ranges of temperature and/or additive molecular weight
13 (M_w) are still questionable. Extra data is still required to generalize these existing prediction
14 models. In this paper, diffusion of a specifically designed homologous set of model additives
15 (from 236 to 1120 g.mol⁻¹) was monitored in two polystyrenes at rubbery state (from 100 to
16 180°C): syndiotactic semi-crystalline polystyrene and its amorphous equivalent. Variations of
17 D and E_a with migrant M_w and temperature were found to be surprisingly low. Comparison
18 of experimental behaviour with model predictions was performed. In their actual form, none
19 of the models is clearly able to describe all experimental data, but clues can be given,
20 showing converging of the different approaches.

21
22 **Keywords:** Diffusion coefficient; FRAP; molecular weight; activation energy; polystyrene;
23 model probes

1 Introduction

2
3
4
5
6
7 To ensure consumer health, food packaging materials must be inert to packaged foodstuffs, in
8
9 order to avoid contamination from harmful substances which can migrate from packaging
10
11 materials. When dealing with plastic, regulations reinforce the concept of an Overall
12
13 Migration Limit (OML) with a Specific Migration Limit (SML) for potentially toxic
14
15 substances filed in a positive list. Petitioners for a new packaging material and control
16
17 authorities have to test polymeric packaging to assess their compliance for food contact (e.g.
18
19 US Food Law Act and EU regulation 2002/72/CE).
20
21

22
23 Migration is kinetically limited by the diffusion step within the polymer matrix, and is
24
25 characterized by the associated diffusion coefficient D . The large amount of diffusion data in
26
27 polyolefins has made the drawing of good prediction models possible. These are useful in
28
29 predicting migration rate into foodstuffs or food simulants. Recently, food safety authorities
30
31 have allowed their use in food packaging material assessments (e.g. art. 4 in EU regulation
32
33 2002/72/CE).
34
35
36
37
38
39

40 *Prediction of diffusion coefficients*

41
42 Different approaches have been developed to model diffusion in polymeric matrixes. From
43
44 Piringer's work, which set up a worst case model (eq. 1) to Limm and Hollifield's model (eq.
45
46 2), the diffusion processes can be simplified and implemented in ready-to-use models.
47
48
49
50
51

$$52 \quad D^* = 10^4 \cdot \exp\left(A_p' - \frac{C}{T} - 0.003M_w \left(45.M_w^{-1/3} - 1\right) - \frac{10454}{T}\right) \quad (1)$$

53
54
55 where D^* is the predicted overestimated diffusion coefficient ($\text{cm}^2 \cdot \text{s}^{-1}$),
56 A_p' and C are tabulated polymer parameters (dimensionless)
57 T is the absolute temperature (K),
58 M_w is the molecular weight of the diffusion species ($\text{g} \cdot \text{mol}^{-1}$).
59
60

$$D(T, M_w) = D'_0 \cdot \exp\left(\alpha \cdot M_w^{1/2} - K \frac{M_w^{1/3}}{T}\right) \quad (2)$$

where D is the predicted diffusion coefficient ($\text{cm}^2 \cdot \text{s}^{-1}$),
 D'_0 is the diffusion coefficient at infinite temperature ($\text{cm}^2 \cdot \text{s}^{-1}$),
 α and K are tabulated polymer parameters (dimensionless),
T is the absolute temperature (K),
 M_w is the molecular weight of the diffusion species ($\text{g} \cdot \text{mol}^{-1}$).

The reliability of such empirical models has been tested (Reynier et al. 1999; Helmroth et al. 2002; Rosca et Vergnaud 2006). Both models are able to describe the diffusion of additives in polyolefins, but prediction errors become significant when dealing with less mobile polymers, or when enlarging the extrapolation range to high temperatures or M_w (Feigenbaum et al. 2005; Dole et al. 2006).

With the goal of creating a more general model, Dole et al. proposed a different approach to predict D with additive molecular weights that try to encompass both mobile and barrier polymers (Figure 1) (Dole et al. 2006). The $D=f(M_w)$ correlations for a broad range of polymers were measured. They then showed that the negative slope of these $[\log_{10}D=f(M_w)]$ correlations decreased from high barrier polymers to lower barrier ones, while the Piringer model uses the same slope for all polymers and the Limm model integrates a weaker dependence. Consequently, as temperature directly affects polymer barrier properties (i.e. matrix mobility), Dole et al. suggested that this high slope variation leads to a variation of apparent E_a with temperature and M_w . The empirical models above can still predict worst case values, but the safety margins may be drastically reduced from polyolefins to other extrapolated systems.

Toward a general predictive model for additive diffusion in polymers?

1 The Dole approach provides a more complex view of diffusion: the $D=f(M_w)$ and $E_a=f(M_w)$
2 slopes are functions of additive M_w but first strongly depend on polymer mobility (Table 1).
3 It is worth noting that both plasticization and T increase allow a barrier polymer to turn into a
4 more mobile one (plasticized vs. non-plasticized PVC, dry vs. 60%RH PA in Figure 1)

5 Piringer's model was built using diffusion coefficients of additives whose M_w was
6 smaller than 500 g.mol^{-1} . Dole et al. studied monitored diffusion of additives whose M_w was
7 up to 807 g.mol^{-1} but with very few data between 430 and 807 g.mol^{-1} . Extrapolation for high
8 M_w additives still needs to be evaluated. In contrast, tabulated parameters in Limm's model
9 were determined by fitting with D of Irganox 1076 (531 g.mol^{-1}) and Irganox 1010 (1178
10 g.mol^{-1}). Therefore, Limm's model may not accurately predict the diffusion of small
11 additives.

12 When dealing with additives of increasing M_w , the overall size, shape, and chemical
13 functionality vary. Therefore, diffusion data of commercial additives are quite scattered.
14 However, the models mentioned above average the molecular size effect by considering only
15 M_w . Up to now, only the Piringer model was validated experimentally against a homologous
16 series of alkanes and alcohols (Reynier et al. 2001; Reynier et al. 2001).

17
18 The same parallel can be drawn for the temperature range. The three models were all
19 built for a specific temperature range. The Piringer model has to be used at a given
20 temperature range depending on the studied polymer (175°C for PET, 70°C maximum for
21 PS). Limm and Hollifield fits α and K parameters between 40 and 70°C . The Dole approach
22 describes diffusion data at 40°C but encompasses a great range of polymer mobility. This
23 model is therefore able to describe diffusion over an equivalent range of temperature. Reynier
24 et al. have shown that diffusion activation by a temperature increase or plasticization fits the
25 general relationship drawn in Figure 1 (Reynier et al. 2001).

1
2
3 1 In order to determine the extent of D dependence on M_w , T- and polymer mobility, it is
4
5 2 still necessary to accumulate D data from homologous systems. This could then help to
6
7 3 determine proper fitting model parameters for barrier polymers and could lead to a general
8
9 4 model.
10
11
12
13
14

15 6 Therefore, this study was set up to follow the diffusion of a specifically designed
16
17 7 homologous set of high M_w probes (Pinte et al. 2008). These probes were chosen to be
18
19 8 probably more accurately model commercial additives than alkanes used by Reynier et al.
20
21 9 (Reynier et al. 2001). Moreover, they are dedicated to the use of the FRAP technique. The
22
23 10 FRAP technique (Fluorescence Recovery After Photobleaching) is a microscopic technique
24
25 11 used to monitor diffusion in both biological samples (Seiffert et Oppermann 2005), and
26
27 12 material ones (Smith 1986; Tseng et al. 2000). It allows the observation of a micro-domain of
28
29 13 the packaging material, without simulant (or food) interactions. This offers a quick
30
31 14 determination of intrinsic apparent diffusion coefficients of model additives, especially when
32
33 15 dealing with low mobility matrixes. The chosen matrix is PS, for which little modelling
34
35 16 validation has been obtained up to now for the following reasons:
36
37
38
39
40

- 41 17 i PS can be either totally amorphous or semi crystalline, depending on its tacticity,
42
43 18 ii It's relatively high glass transition temperature (T_g) facilitates measurements in
44
45 19 the vicinity of T_g , even at a glassy state,
46
47
48 20 iii PS displays a large rubbery plateau without any important structural change
49
50 21 (cold crystallization, melting). As a crystalline PS, syndiotactic PS (sPS) was
51
52 22 preferred to isotactic PS because of its higher cold-crystallization and melting
53
54 23 temperatures. When correctly annealed, sPS shows no post-crystallization or
55
56 24 melting over the studied range of temperatures (100 to 180 °C).
57
58
59
60

To resume, the relationships $D=f(M_w)$ and $D=f(1/T)$ are established and discussed in this paper. Effects of crystallinity are also discussed. Comparison of experimental behavior with model predictions is made.

Material and methods

Material

Amorphous atactic model polystyrene PS2M was obtained as a SEC (steric exclusion chromatography) standard from Sigma Aldrich (Saint Quentin Fallavier, France):

$\overline{M}_w = 1\,850\,000\text{ g}\cdot\text{mol}^{-1}$, $\overline{M}_n = 1\,760\,000\text{ g}\cdot\text{mol}^{-1}$, $\overline{M}_w / \overline{M}_n = 1.05$. Syndiotactic polystyrene was purchased from Scientific Polymer Products (Ontario, USA): approx. $\overline{M}_w = 300\,000\text{ g}\cdot\text{mol}^{-1}$, density=1.05.

The series of fluorescent probes was synthesized as previously described (Pinte et al. 2008). This set of five homologous molecules, as shown in table 2, was made by grafting a fluorescent head (7-nitrobenzofurazan) onto an amino acid-like tail. This “tail” was synthesized by oligomerization of the same repeating unit. Tail molecular weight was increased by repeating the same ‘monomer-like’ unit. For more detailed synthetic procedures, please refer to the above mentioned article and its *Supporting Information*.

Methods

Both polymers were characterized by differential scanning calorimetry (MDSC 2940, TA Instruments). The heating rate was $10\text{K}\cdot\text{min}^{-1}$. Glass transition temperatures were determined as the inflection point of heat flow from the second run, whereas melting temperature and melting enthalpy were determined from the first run. For sPS, crystallinity was found to be 70%, assuming a heat of fusion of $53\text{ J}\cdot\text{mol}^{-1}$ (Bruzard et al. 2005). Both thermograms are shown in figure 2.

1
2
3
4 1
5 2 Films of amorphous polystyrene for FRAP experiments (PS2M) were made as described in
6
7 3 (Pinte et al. 2008) by casting from an ethyl acetate solution onto a cover slide, followed by
8
9
10 4 solvent evaporation under dynamic vacuum at 90 °C, The cover slides were then mounted onto a
11
12 5 microscope slide by slight pressure and heating at 120 °C for several seconds. sPS is non soluble in
13
14 6 the same systems as aPS. Therefore, samples were made using the following method:

- 15
16
17 7 i dissolution in a refluxed toluene solution containing the proper amount of the
18
19 8 fluorescent probe,
20
21 9 ii casting on a hot plate (100 °C) to allow quick evaporation of toluene and to
22
23 10 avoid sPS precipitation,
24
25 11 iii removal of toluene traces at 90 °C in a dynamic vacuum oven for two days,
26
27 12 iv pressing a small piece of doped sPS between a glass microscope slide and a
28
29 13 glass cover slide at 270 °C.
30
31
32

33 14 In order to have fixed crystallinity sPS samples, sPS slides were annealed at 270 °C for
34
35 15 2 minutes and cooled at constant rate of 10 °C.min⁻¹ to allow crystallization to occur.
36
37

38 16 DSC showed no cold crystallization peak when heating these samples above T_g, up to
39
40 17 melting point.
41
42
43
44

45 19 Fluorescent probe diffusion was monitored by confocal Fluorescence Recovery After
46
47 20 Photobleaching (FRAP) as described elsewhere (Pinte et al. 2008). This microscopic
48
49 21 technique has been previously used as a relevant method to collect D data in polymers (Smith
50
51 22 1986). FRAP creates an *in situ* concentration gradient in the bulk of small polymer samples.
52
53 23 The flux of the fluorescent species then induces an intensity fluctuation over the Region of
54
55 24 interest (ROI). From a practical point of view, FRAP experiments are conducted in three
56
57 25 steps: (i) reading the initial intensity with low laser power, (ii) bleaching a specified area by
58
59 26 scanning a selected region of the sample (the ROI) with very high laser power, thus
60

1 photolysing the illuminated fluorescent probe, (iii) reading the recovery of the fluorescence
2 intensity over time with low laser power. As intensity is assumed to be proportional to local
3 probe concentration, D can be calculated from the fluorescence recovery kinetics. The
4 bleached ROIs were ranging from $1.5 \times 20 \mu\text{m}$ for low diffusing experiments to $67 \times 61 \mu\text{m}$
5 for diffusion at high temperatures.

6 The Shape ratio of the different probes used for FRAP experiment, denoting the ratio of a
7 migrant's major dimension to its minor dimension was determined from NBDNet2 to
8 NBDNpip4. By 3D-drawing the molecules using MarvinSpace (software from ChemAxon),
9 both dimension of the molecules then the shape ratio were easily determined.

10 Experiments were set at a higher temperature than allowed on the microscope sample
11 holder. Therefore, sample slides were mounted once for reading and bleaching, then
12 demounted to be heated between two hot plates of a heating press, cooled down as quickly as
13 possible and remounted to read the fluorescence profile evolution. The last steps were
14 repeated until ROI intensity had varied enough to calculate D . Since the sample requires time
15 to reach thermal equilibrium under the press, diffusion time (i.e. time spent in the heating
16 press) was corrected to take this into account, assuming diffusion at lower temperatures to be
17 negligible.

18 To help re-localization in the sample when re-mounting under the confocal microscope,
19 thin copper grids (Oxford Instruments, Saclay, France) were immersed in the PS in the casted
20 drop of PS2M or in the molten piece of sPS. The hexagonal pattern (figure 3) provides
21 valuable information when saved coordinates failed to precisely point to the region of
22 interest. Due to the high temperatures required for the experiments, sandwiches of slides/PS
23 sample/coverglass were sealed with epoxy glue instead of nail polish.

24

1 FRAP kinetics were processed as described elsewhere (Pinte et al. 2008). Due to quick
2 diffusion (as high temperatures were explored), bleached ROIs were enlarged to extend
3 recovery timescales. Unfortunately, bleaching was not efficient enough in the depth of the
4 sample and apparent anomalous fluorescence recovery had to be corrected. As a consequence,
5 the mathematical analysis implemented by Pinte et al. was slightly modified to eliminate this
6 unwanted diffusion from planes below and above the focal plane and to analyze fluorescence
7 recovery due to x-axis 1D diffusion.

8 Several authors using the FRAP method have reported immobile fractions when
9 monitoring diffusion in complex systems (Miura 2004, Karboviak et al. 2006).
10 Consequentially, equilibrium intensity in the bleached area may not be the same as in the
11 initial one. The ratio of the final intensity to the initial one represents the percentage of
12 mobile probes. The difference between this value and 100% then gives the amount of non
13 mobile probes. Our diffusion experiments in syndiotactic polystyrene were therefore first
14 conducted for a much longer time (6 months) than in the usual procedure in order to estimate
15 the equilibrium intensity.

17 **Results and discussion**

18 PS samples containing the probes (5×10^{-10} mol.mg⁻¹) were obtained. All probes were
19 correctly dispersed in the polymer matrixes, notwithstanding whether these were amorphous
20 or crystalline. However, some patterns were observed in sPS, revealing the partial exclusion
21 of fluorescent probes from more crystalline regions. This did not disturb FRAP experiments
22 and diffusion of the different items of the homologous set was monitored in PS2M and in sPS
23 for different temperatures ranging from 120 to 180 °C.

1 Literature on the FRAP technique mentions that in the case of complex polymer
2 systems, fluorescence recovery may not be total which is to be taken into account in the D
3 calculation. For example, Equilibrium intensity is lower, denoting non mobile probes. This is
4 supposed to be the case in semi-crystalline polymers where some of the probes could be
5 entrapped and not available for diffusion. This was checked in this study but no immobile
6 fraction was observed, even if some patterns could be observed in sPS samples (figure 3-
7 sPS). Diffusion was found to be very similar in PS2M and in sPS. Equilibrium intensities
8 were not different and close to the initial ones (less than a 10% decrease). Crystallinity did
9 not induce a bigger change in mobile/non mobile probe ratios. Therefore, initial intensities
10 were used as equilibrium intensities.

12 Diffusion coefficients were measured for the five homologous probes, whose M_w
13 ranged from 236 to 1120 $\text{g}\cdot\text{mol}^{-1}$, in both amorphous and semi-crystalline PS, with an
14 experimental temperature increases from 100 °C to 180 °C. Those for PS2M are reported in
15 table 3.

17 *$[\log_{10}D=f(M_w)]$ correlations*

18 Diffusion coefficients as a function of M_w for different temperatures are plotted on Figure 4.
19 The total decrease of $\log_{10}D$ with M_w for different temperatures is shown in table 3.
20 Increasing M_w from 236 to 1120 $\text{g}\cdot\text{mol}^{-1}$ lead to a decrease of about two units of $\log_{10}D$ for
21 all the tested temperatures. Indeed, as shown in figure 4, an arbitrary line can fit all data at
22 rubbery state, by only vertical shifts as lines are parallel. As reported in Table 3, the slope can
23 be considered as almost constant, when not taking into account data at 100°C. The slope
24 seemed smaller at 100°C, when PS2M is at its DSC glass transition temperature.

1
2
3 1 The constancy of the $\log_{10}D = f(M_w)$ slope correlations relates the PS2M data to the
4
5 2 Piringer model, where influence of M_w and T on D are independent. The D decrease is quite
6
7 3 small (roughly from 1 to 2 orders of magnitude) for an 890 g.mol^{-1} increase of the migrant
8
9 4 molecular weight. For example, Reynier et al. reported a 4orderofmagnitude decrease for
10
11 5 diffusion in polyolefins over the same range but for lower M_w (from 156 to 807 g.mol^{-1})
12
13 6 (Reynier et al. 2001). But , the first molecule of the homologous series used in this study has
14
15 7 a higher M_w compared to Reynier et al.'s one which was made for a migrant molecular
16
17 8 weight between Npip2 and Npip3. As reported by Dole et al., the sharp decrease observed
18
19 9 for D mainly occurs for rather low M_w that is to say between gases and small additives (M_w
20
21 10 less than 200 g.mol^{-1}). For higher molecular weight additives, extrapolation of such $D =$
22
23 11 $f(M_w)$ curves could leads, in the present study, to a flatter slope of $D=f(M_w)$ (Dole et al.
24
25 12 2006).

26
27 13 Migrant shape (steric hindrance) is known to be a limiting parameter for diffusion,
28
29 14 whereas increasing migrant degrees of freedom counterbalances this by increasing diffusion
30
31 15 (Al-Malaika et al. 1991). Reynier has reported a high decrease as predicted by the Piringer
32
33 16 model when taking into account homologous series of both alkanes and alcohols as well as
34
35 17 commercial additives for higher M_w (Reynier et al. 2001). They observed that for high M_w
36
37 18 migrants, increasing the degrees of freedom of the arms lead to a relative increase of D
38
39 19 (trilaurine and tripalmitine with long alkyl arms compared to Irgafos 168 and Irganox 1330,
40
41 20 with highly hindered arms). In fact, in our study, D decrease with migrant M_w is rather low
42
43 21 as reported above. This can be explained by the model additives series which are not shape-
44
45 22 homologous over the whole range of M_w (as initially expected) . Although they all have a
46
47 23 worm-like shape (shape ratio <1 as shown in figure 5), and due to the repet unit (table 3), this
48
49 24 ratio decreases along the series: NBDNet₂ has a more spherical shape than NBDNpip_n.
50
51 25 Moreover, when jumping from NBDNet₂ to NBDNpip₁, no extra degree of freedom is added,
52
53
54
55
56
57
58
59
60

1 in contrast to the change from $NBDN_{pip_n}$ to $NBDN_{pip_{n+1}}$, where the migrant linearity is
2 improved. This provides extra degrees of freedom when increasing migrant M_w and thus, the
3 influence of shape through M_w on D seems to be minimized.

4 The Piringer model implies a much higher dependence of D on M_w (between $NBDNet_2$
5 and $NBDN_{pip_4}$, $\Delta \log_{10} D = 6.75$ instead of about 2 in this study). Extrapolation of the Limm
6 model and the Dole approach to higher temperatures predicts variations closer to those
7 observed in this study (respective predicted decrease $\Delta \log_{10} D$ of 2.75 and 3). D values have
8 been reported to be less dependent on M_w in rubbery polymers than in more barrier ones
9 (Dole et al. 2006). But the flatter slope, (figure 4), at 100 °C gives the opposite indication as
10 predicted by Dole et al.

12 *D=f(1/T) correlations*

13 In consistency with any migration model, D was found to increase when increasing
14 temperature as shown in figure 6. The different D values between 120 °C and 180 °C ranged
15 from 3.2 to 3.9 $\log_{10} D$ units (table 3).

16 Close to glass transition, D variations are emphasized. Although requiring further
17 confirmation, the higher the M_w , the stronger the dependence with T . For $NBDNet_2$ to
18 $NBDN_{pip_3}$, the D jump temperature is between 100 and 120 °C whereas for $NBDN_{pip_4}$, it
19 occurs at a higher temperature (the jump is related to the D data which leave the $D = f(M_w)$
20 line observed at high temperature). The T_g jump seems to be a function of M_w , as it is of
21 frequencies or heating speed in thermo-mechanical analysis (Sauerbrunn et al. 2003).
22 Activation energies (E_a) are calculated from the Arrhenius law as usually describes by others
23 authors (Hayashi et al. 1994, Roe et al. 1998). E_a is then proportional to the slope of the curves
24 $\log D = f(1/T)$ and determine from the least squares approach. For homogeneity, activation

1
2
3 1 energies were calculated between 120 and 180 °C, assuming they are constant over this range
4
5 2 of temperature.
6
7

8 3 E_a are between 140 and 180 °C slightly increased with molecular weight (table 4),
9
10 4 whereas between 120 and 180 °C, it could be considered as constant, considering the data
11
12 5 scattering . Results on a reduced range limit comparison with the Piringier model, which takes
13
14 6 a constant E_a into account, and make the PS2M data closer to the Limm and Hollifield model
15
16 7 (respective increase of E_a from Net_2 to Npip_4 is 1.5 vs 1.7). The effect of M_w seems to prevail
17
18 8 over the shape factor ratio, in contrast to diffusion coefficients. This odd behavior, however,
19
20 9 makes one relationship clear: the weaker the dependence of the $D=f(M_w)$ slope with
21
22 10 temperature, the smaller E_a variations.
23
24
25

26
27 11 Increasing linearity for higher M_w leads to a weaker shape factor influence and
28
29 12 therefore decreasing dependence of E_a with M_w .
30
31
32
33

34 14 E_a were then compared to data in rubbery PS and LDPE. Hall et al. studied the diffusion
35
36 15 of lophine in rubbery PS between 100 and 145 °C. (Hall et al. 1999). From their data, the
37
38 16 calculated E_a ($272 \text{ kJ}\cdot\text{mol}^{-1}$) is one and a half times larger than Hall et al.'s equivalent E_a
39
40 17 (M_w of lophine is between that of NBDNet_2 and NBDNpip_1). This difference may lie in the
41
42 18 different shape and degree of freedom. As previously mentioned, the homologous set is worm
43
44 19 shaped with a propyl spacer between rigid cores providing degrees of freedom, whereas
45
46 20 lophine is more spherical with three short and rigid phenyl arms. This difference in E_a s is
47
48 21 logical because the E_a represents the energy required to open a sufficient hole between
49
50 22 polymer chains for the migrant to diffuse: thus, a greater probe diameter means a higher E_a
51
52 23 (Al-Malaika et al. 1991; Reynier et al. 2001). However, these reported E_a s are very high
53
54 24 compared to those calculated by Al-Malaika et al. (Al-Malaika et al. 1991) for homologous
55
56 25 linear 2-hydroxy benzophenones in LDPE (between 69 and $86 \text{ kJ}\cdot\text{mol}^{-1}$ from 5 to 100 °C).
57
58
59
60

1 This could be explain by the mobility of the matrix: the temperature gap to the T_g is far
2 bigger in Al-Malaika's experiment (for LDPE: T-T_g ~ 150 °C) than in ours (0 < T-T_g < 80
3 °C) or in Hall's (0 < T-T_g < 45 °C). This corroborates the suggestion of Dole et al. (Dole et
4 al. 2006) that E_a may decrease with increasing temperature, but over a larger range and
5 farther from the T_g than studied here.

6 *D=f(crystallinity)*

7 Crystallinity is reported to decrease D by hampering migrant diffusion as described by
8 Hedenqvist et al. (Hedenqvist et al. 1996). Some authors even describe an exponential
9 relationship between D and cristallinity (Klopffer and Flaconnèche 2001).

10
11
12 Hedenqvist et al. report a five-fold reduction of D in linear PE and a two-fold one in
13 branched PE when increasing crystallinity by 50% (Hedenqvist et al. 1996). The same
14 observation was made by Chiang et al. when comparing quenched pseudo amorphous sPS
15 with isothermally crystallized sPS (Chiang et al. 2002). Such reductions are of the same
16 magnitude of what was found in our system (Figure 7). Nevertheless, larger D_s in sPS than in
17 PS2M at low temperature are odd. (from Figure 7 and other results not shown). In addition,
18 no increasing difference between D_{amorphous} and D_{crystalline} with the additive M_w was found, in
19 contrast to what Hedenqvist et al. reported. The torturous diffusion path in sPS might be
20 counterbalanced by the increase of free volume due to increased tacticity and T_g heights.
21 Highly tactic polymers have been reported to have higher free volume than atactic ones due to
22 special chain conformation (Dammert et al. 1999; Soldera et Grohens 2002). When getting
23 close enough to T_g, tortuosity effect may become less important than free volume size and
24 chain mobility.

1 **Conclusions**

2 Diffusion in two different PS, one amorphous and one semi-crystalline, was monitored at the
3 rubbery state for five homologous probes, offering a M_w range of almost $900 \text{ g}\cdot\text{mol}^{-1}$.
4 Diffusion was found to be less dependent on temperature or migrant molecular weight than
5 calculated from prediction models.. However, D decrease for M_w range was found close to
6 the Limm model. This low dependence might be explained by the higher M_w of the first
7 molecule of the model migrant series. Another hypothesis may be offered to explain the low
8 correlation between D and M_w . Even if the probes are chemically homologous, they are
9 unfortunately not ideally homologous; their shape factor varies along the series from
10 relatively square to worm-like. This variation may counteract the decrease of D as M_w gets
11 higher. Bearing this fact in mind, none of the models can be excluded, based on the study's
12 data. Moreover, all the three models can partially explain the observed effects of M_w and T
13 on D.

14 Whatever hypothesis is taken into account, the following general relationship is
15 accurate: when D is not strongly affected by M_w or T, neither is E_a . Further experiments are
16 required to develop a general model for: (i) a more shape-homologous series of designed
17 migrants, and (ii) diffusion in glassy matrices, where very little data are still available because
18 of very long diffusion time The Frap technique could help to acquire information about that
19 issue.

References

- Al-Malaika, S., Goonetilleka, M.D.R.J., Scott, G. (1991) Migration of 4-substituted 2-hydroxy benzophenones in low density polyethylene: Part I-Diffusion characteristics. *Polymer Degradation and Stability* 32(2), pp 231-247.
- Bruzaud,S., Grohens Y., Ilinca S., Carpentier J.F.(2005). Syndiotactic Polystyrene/Organoclay Nanocomposites: Synthesis via In Situ Coordination-Insertion Polymerization and Preliminary Characterization. *Macromolecular Materials and Engineering* 290(11), pp1106-1114.
- Chiang, I. J., Chau C. C., Sanboh L. (2002). The mass transport of ethyl acetate in syndiotactic polystyrene. *Polymer Engineering & Science* 42(4), pp724-732.
- Dammert, R. M., Maunu, S. L., Maurer, F.H. J., Neelov, I.M., Niemela, S., Sundholm, F., Wastlund, C.(1999). "Free Volume and Tacticity in Polystyrenes." *Macromolecules* 32(6), pp1930-1938.
- Dole, P., Feigenbaum A.E., Dole, P., De La Cruz, C., Pastorelli, S., Paseiro, P., Hankemeier, T., Voulzatis, Y., Aucejo, S., Saillard, P., Papaspyrides, C. (2006). Typical diffusion behaviour in packaging polymers: application to functional barriers. *Food Additives & Contaminants* 23(2), pp 202-211.
- Feigenbaum, A., P. Dole, Aucejo, S., Dainelli, D., Garcia, C., De La Cruz, Hankemeier, T., Ngono, Y., Papaspyrides, C. D., Paseiro, P., Pastorelli, S., Pavlidou, S., Pennarun, P. Y., Saillard, P., Vidal, L., Vitrac, O.Voulzatis, Y. (2005). Functional barriers: Properties and evaluation. *Food Additives & Contaminants* 22(10), pp 956-967.
- Hall, D. B., Hamilton K. E., Miller, R. D.,Torkelson, J.M. (1999). Translational and Rotational Diffusion of Probe Molecules in Polymer Films near Tg: Effect of Hydrogen Bonding. *Macromolecules* 32(24), pp 8052-8058.
- Hayashi H, Sakai H., Matsuzawa S. (1994). Diffusion of methyesters of higher fatty acid in polypropylene. *Journal of applied polymer science*. 51, pp2165-2173.

- 1
2
3 1
4
5 2 Hedenqvist, M., Angelstok A. (1996). Diffusion of small-molecule penetrants in
6
7 3 polyethylene: free volume and morphology. *Polymer* 37(14), pp2887-2902.
8
9 4
10 5 Helmroth, E., Rijk R., , Dekker, M., Jongen, W. (2002). Predictive modelling of migration
11
12 6 from packaging materials into food products for regulatory purposes. *Trends in Food Science*
13
14 7 & *Technology* 13(3), pp102-109.
15
16 8
17 9 Karboviak, T., Hervet H., (2006). Effect of plasticisers (water and glycerol) on the diffusion
18
19 10 of a small molecule in Iota-carrageenan biopolymer films for edible coating application.
20
21 11 *Biomacromolecules* 7(6), pp 2011-2019
22
23 12 Klopffer, M. H. and B. Flaconneche (2001). Transport Properties of Gases in Polymers:
24
25 13 Bibliographic Review. *Oil & Gas Science and Technology* 56(3), pp 223-244.
26
27 14
28 15 Miura, K. (2004). What do FRAP curves tell us ?. EAMNET practical course, Heidelberg,
29
30 16 AMBL Heidelberg.
31
32 17
33 18 Pinte, J., Joly C., , Plé, K., Dole, P., Feigenbaum, A. (2008). Proposal of a Set of Model
34
35 19 Polymer Additives Designed for Confocal FRAP Diffusion Experiments. *Journal of*
36
37 20 *Agricultural and Food Chemistry* 56(21), pp 10003-10011.
38
39 21
40 22 Reynier, A., Dole, P., Feigenbaum, A. (1999). Prediction of worst case migration:
41
42 23 presentation of a rigorous methodology. *Food Additives and Contaminants* 16, pp137-152.
43
44 24
45 25 Reynier, A., P. Dole, et al. (2001). "Additive diffusion coefficients in polyolefins. II. Effect of
46
47 26 swelling and temperature on the $D = f(M)$ correlation." *Journal of Applied Polymer Science*
48
49 27 82(10), pp 2434-2443.
50
51 28
52
53 29 Reynier, A., Dole P., Humbel S., Feigenbaum A., (2001). Diffusion Coefficients of Additives
54
55 30 in Polymers. I. Correlation with Geometric Parameters. *Journal of Applied Polymer Science*
56
57 31 82(10), pp 2422-2433.
58
59 32
60 33 Roe R.J., Bair H., Gieniewsky C. (1974). Solubility and diffusion coefficient of antioxidants
34 in polyethylene. *Journal of polymer science*, 18, pp 843-856.

- 1
2
3 1
4
5 2 Rosca, I. D. and Vergnaud J. M. (2006). Approach for a testing system to evaluate food safety
6 with polymer packages. *Polymer Testing* 25(4), pp 532-543.
7
8 4
9
10 5 Sauerbrunn, S., Riesen R., (2003). Glass transition by DSC, TMA and DMA. NATAS Annual
11 Conference on Thermal Analysis and Applications, Albuquerque, NATAS.
12
13 7
14
15 8 Seiffert, S. and W. Oppermann (2005). Systematic evaluation of FRAP experiments
16 performed in a confocal laser scanning microscope. *Journal of Microscopy* 220(1): 20-30.
17
18 9
19 10
20
21 11 Smith, B. A. (1986). Photochemical Methods for Measuring Polymer Diffusion.
22 *Photophysical and photochemical Tools in Polymer Science*. M. A. Winnik, D. Reidel
23 Publishing Company, pp 397-406.
24
25 13
26 14
27
28 15 Soldera, A. and Y. Grohens (2002). Molecular modeling of the glass transition of
29 stereoregular PMMAs. *Polymer-Plastics Technology and Engineering* 41(3), pp561 - 571.
30
31 17
32
33 18 Tseng, K. C., Turro N. J., , Durning, C. J. (2000). Tracer diffusion in thin polystyrene films.
34 *Polymer* 41(12), pp 4751-4755.
35
36 19
37 20
38 21
39
40
41
42
43
44
45
46
47
48
49
50
51
52
53
54
55
56
57
58
59
60




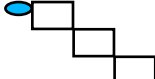
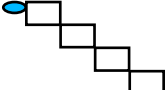
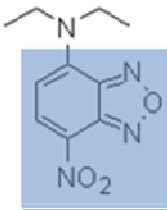
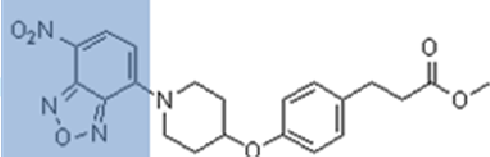
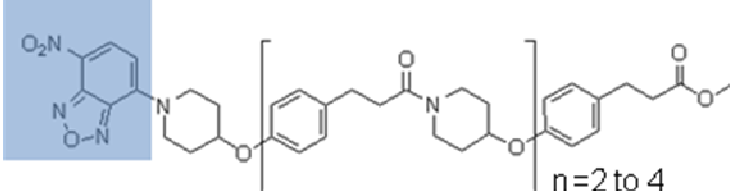
1
2
3 **Table 1. Factors influencing diffusion coefficients and activation energies according to the three models**
4
5
6

7

Model	D influencing factors			Ea influencing factors		
Piringer's model	M_w	T	<i>polymer</i>	<i>polymer</i>		
Limm and Hollifield's model	M_w	T	<i>polymer</i>	polymer	M _w	
Dole's model	polymer	M _w	T	M_w	polymer	T

8
9
10
11
12
13
14
15
16
17 3 strong dependence (bold), average dependence (normal), weak dependence (*italic*)
18
19
20
21
22
23
24
25
26
27
28
29
30
31
32
33
34
35
36
37
38
39
40
41
42
43
44
45
46
47
48
49
50
51
52
53
54
55
56
57
58
59
60

1 **Table 2. Characteristics and structures of the homologous fluorescent set of model additives.**

Name	NBDNEt ₂	NBDNpip ₁	NBDNpip ₂	NBDNpip ₃	NBDNpip ₄
n (number of 'monomer' units)	0	1	2	3	4
Structure					
M _w (g.mol ⁻¹)	236	426	658	889	1120
NBDNEt ₂					
NBDpip ₁					
NBDpip _(2 to 4)					

2 The filled elliptical head and open rectangles represent the NBD chromophore (in blue) and repeating units (pip)

3 respectively.

1
2
3
4
5
6
7
8
9
10
11
12
13
14
15
16
17
18
19
20
21
22
23
24
25
26
27
28
29
30
31
32
33
34
35
36
37
38
39
40
41
42
43
44
45
46
47
48
49
50
51
52
53
54
55
56
57
58
59
60

1
2

Table 3. Diffusion coefficients measured in amorphous polystyrene (PS2M) at various temperatures (D are in $10^{-12} \text{ cm}^2 \cdot \text{s}^{-1}$). Probes legend are given in table 2.

Probes		Temperature ($^{\circ}\text{C}$)					
	M_w ($\text{g} \cdot \text{mol}^{-1}$)	180	160	140	120	100	$\Delta \log_{10} D^b$
N Et_2	236	17000	1400	48	9,5	0,026	3.2
Npip ₁	426	12000	1000	60	7,0	0,0081	3.2
Npip ₂	658	5100	480	4	0,64	nd	3.9
Npip ₃	889	600	140	10	0, 29	0,0035	3.3
Npip ₄	1120	500	84	0,13	0.07	0,0008	3.8
$\Delta \log_{10} D^a$		-1.5	-1.2	-2.6	-2.1	-1.2	

3
4

^a $\Delta \log_{10} D$ were calculated from NBDN Et_2 to NBDNpip₄

^b $\Delta \log_{10} D$ were calculated between 120 $^{\circ}\text{C}$ and 180 $^{\circ}\text{C}$

Table 4. Calculated activation energies (E_a) for the model additives in atactic polystyrene (PS2M). Arrhenius plot of PS2M diffusion coefficients.

Model additive	M_w (g.mol ⁻¹)	E_a (kJ.mol ⁻¹)	
		between 120 and 180 °C	between 140 and 180 °C
Net ₂	236	187	170
Npip ₁	436	189	179
Npip ₂	658	219	237
Npip ₃	889	188	212
Npip ₄	1120	239	249

E_a were calculated assuming an Arrhenian behavior and a constant E_a between 120 and 180 °C.

For Peer Review Only

Figure captions

Figure 1. Diffusive behaviour of different migrants in polymers at 40°C, redrawn from Dole et al.'s data (Dole et al. 2006).

Circles refer to diffusion in mobile polymers, such as LLDPE, LDPE, plasticized PVC, plasticized PP), triangles show D for barrier polymers (dry PA, dry EVOH, unplasticized PVC, PET, PMMA, PS), and squares refer to intermediate polymers (PA at 60%RH, PP). Diffusion was carried out at 40°C. The arrow indicates an increasing matrix mobility, embodied by the system glass transition temperature.

Figure 2. Thermal characterization of virgin PS2M (atactic polystyrene) and sPS (semicrystalline syndiotactic polystyrene sPS)

Figure 3. syndiotactic polystyrene (sPS sample), showing non homogeneously dispersed Npip2 probes (left), and homogeneous dispersion in amorphous polystyrene PS2M (right). Zoom: 1.9, picture size: 125x125 µm. The black pattern of the copper hexagonal grid can be seen immersed in the sPS sample.

Figure 4. Diffusion coefficients in PS2M as a function of M_w for different temperatures.

Plain lines have the same slope, they are vertically shifted to best describe $D=f(M_w)$ for each temperature. The dotted line ($T=100^\circ\text{C}$) has a different slope.

Figure 5. Shape ratio of the different probes used for FRAP experiment, from NBDNet₂ to NBDNpip₄.

The dimension ratio, which is equal to the largest cross section from head to tail, was estimated by drawing the molecules in MarvinSpace (ChemAxon).

Figure 6. Arrhenius plot of PS2M diffusion coefficients.

1
2
3 1 Lines are drawn only as guides. The dotted line (Npip4), however, has a lower slope than
4 2 other plain lines.
5
6
7
8 3

9
10 4 **Figure 7. Comparison of the diffusion of two probes in amorphous or semi crystalline**
11 5 **polystyrenes.**
12
13
14
15
16
17
18
19
20
21
22
23
24
25
26
27
28
29
30
31
32
33
34
35
36
37
38
39
40
41
42
43
44
45
46
47
48
49
50
51
52
53
54
55
56
57
58
59
60

For Peer Review Only

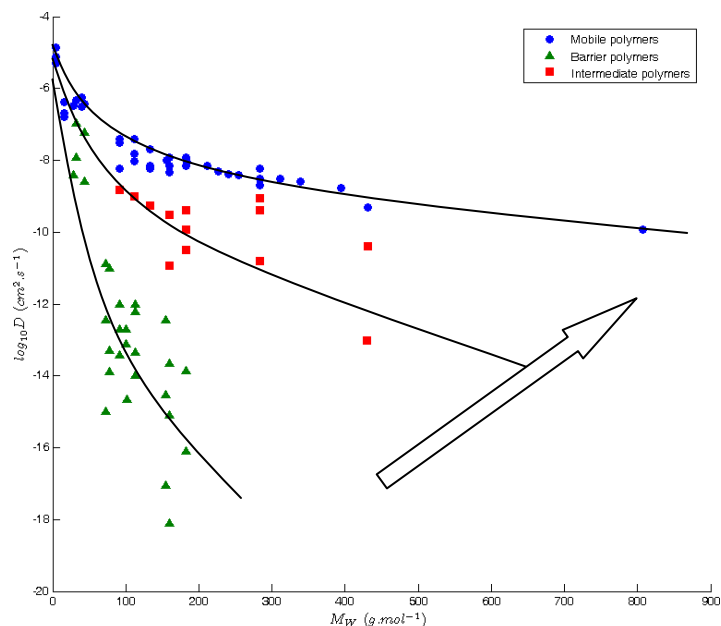


Figure 1. Diffusive behaviour of different migrants in polymers at 40°C, redrawn from Dole et al.'s data (Dole et al. 2006).

Circles refer to diffusion in mobile polymers, such as LLDPE, LDPE, plasticized PVC, plasticized PP), triangles show D for barrier polymers (dry PA, dry EVOH, unplasticized PVC, PET, PMMA, PS), and squares refer to intermediate polymers (PA at 60%RH, PP). Diffusion was carried out at 40°C. The arrow indicates an increasing matrix mobility, embodied by the system glass transition temperature.

1
2
3
4
5
6
7

view Only

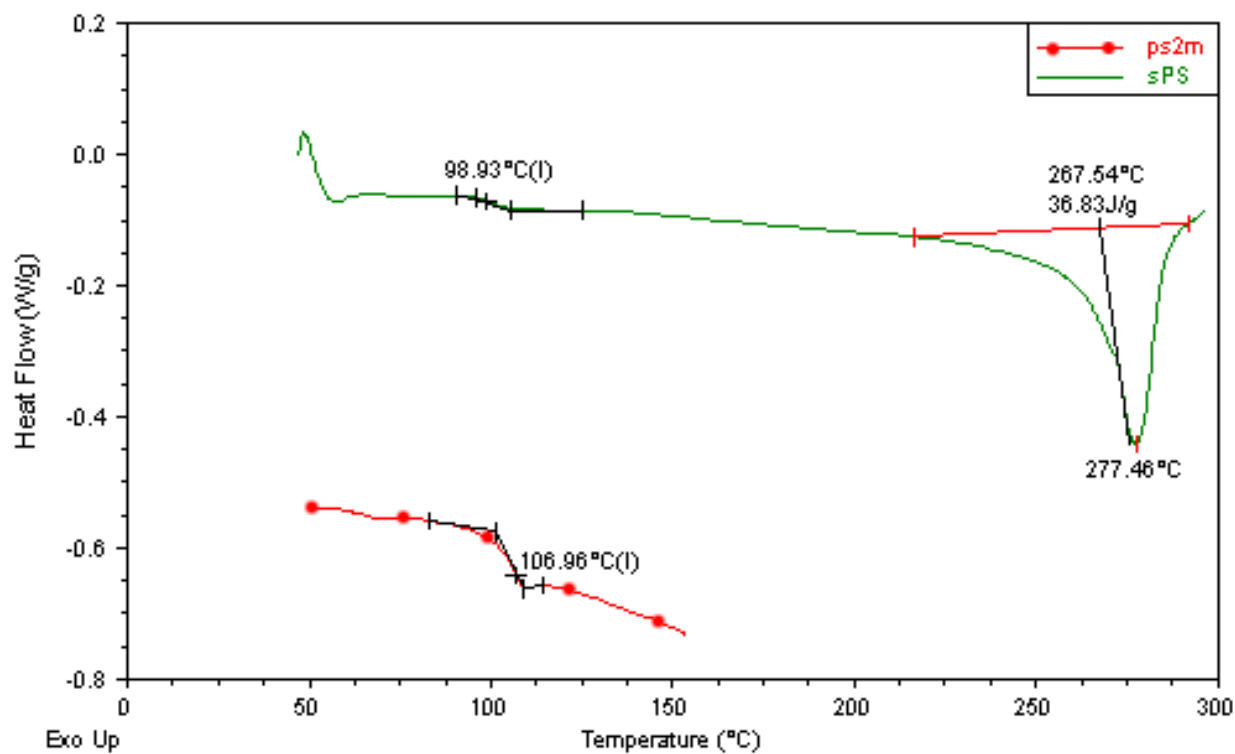
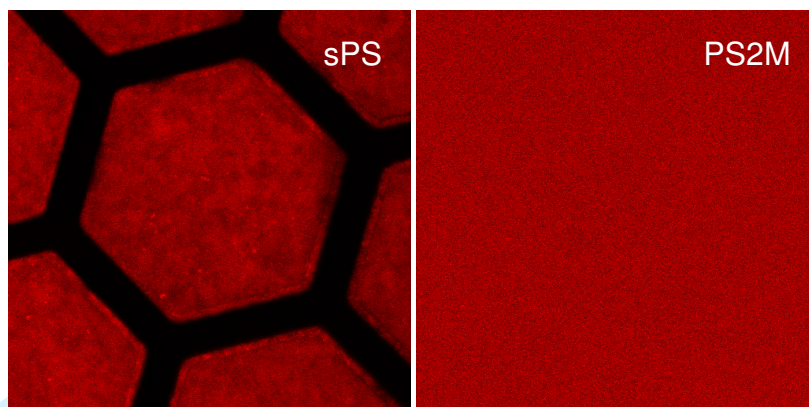


Figure 2. Thermal characterization of virgin amorphous polystyrene (PS2M) and semi crystalline polystyrene (sPS)



1
2
3
4
5
6
7
8
9
10
11
12
13
14
15
16
17
18
19
20
21
22
23
24
25
26
27
28
29
30
31
32
33
34
35
36
37
38
39
40
41
42
43
44
45
46
47
48
49
50
51
52
53
54
55
56
57
58
59
60

1 Figure 3. Semi-cristallilne polystyrene (sPS) sample, showing non homogeneously dispersed Npip2 probes
2 (left), and homogeneous dispersion in amorphous polystyrene (PS2M) (right). Zoom: 1.9, picture size:
3 125x125 μm . The black pattern of the copper hexagonal grid can be seen immersed in the sPS sample.

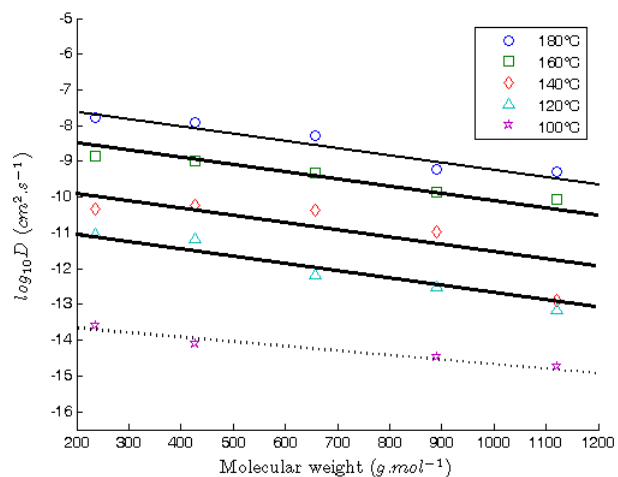


Figure 4. Diffusion coefficients in amorphous polystyrene (PS2M) as a function of probes M_w for different temperatures.

Plain lines have the same slope, they are vertically shifted to best describe $D=f(M_w)$ for each temperature. The dotted line ($T=100^\circ\text{C}$) has a different slope.

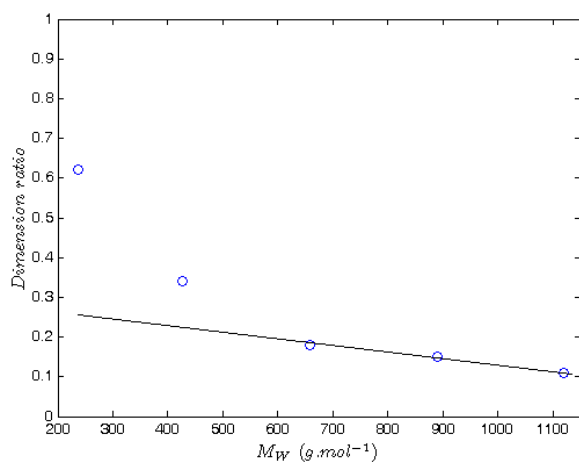


Figure 5. Shape ratio of the different probes used for FRAP experiment, from NBDNET₂ to NBDNpip₄ ‘see tables 2 for probe chemical structures)

The dimension ratio, which is equal to the largest cross section from head to tail, was estimated by drawing the molecules in MarvinSpace (ChemAxon).

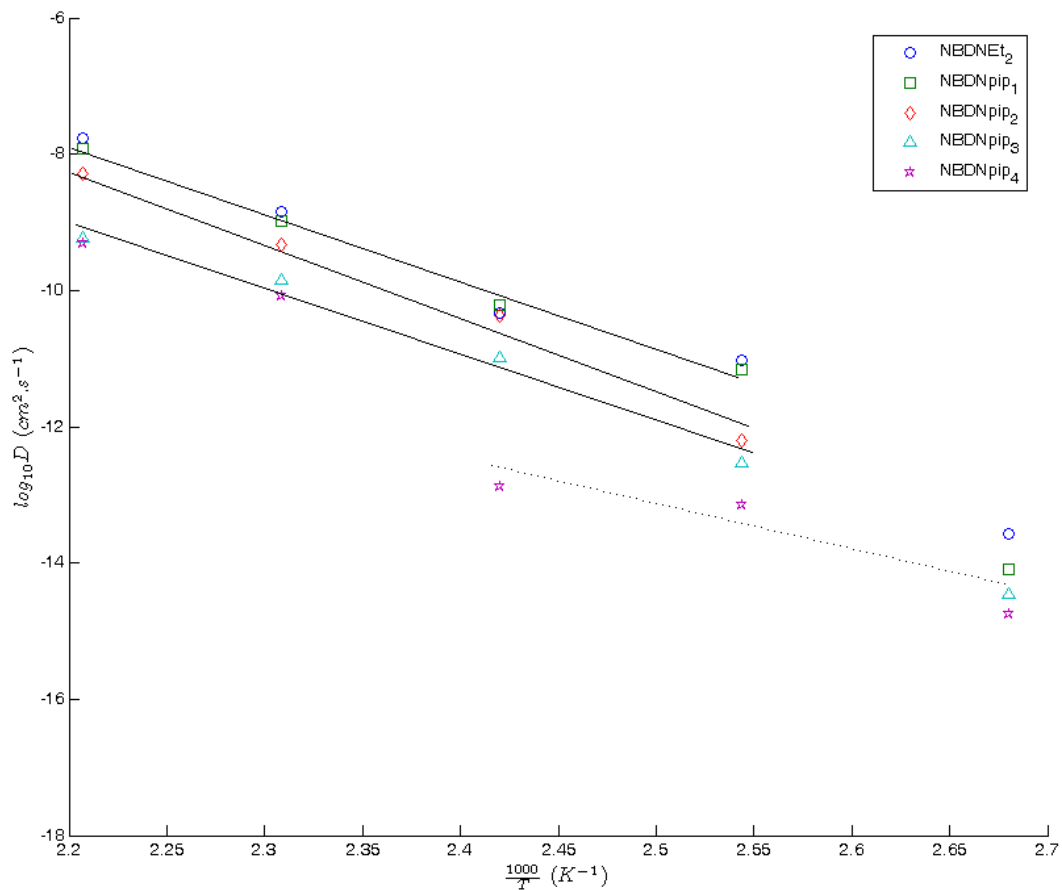


Figure 6. Arrhenius plot of amorphous polystyrene (PS2M) diffusion coefficients. Probes legend is given in table 2.

Lines are drawn only as guides. The dotted line (Npip4), however, has a lower slope than other

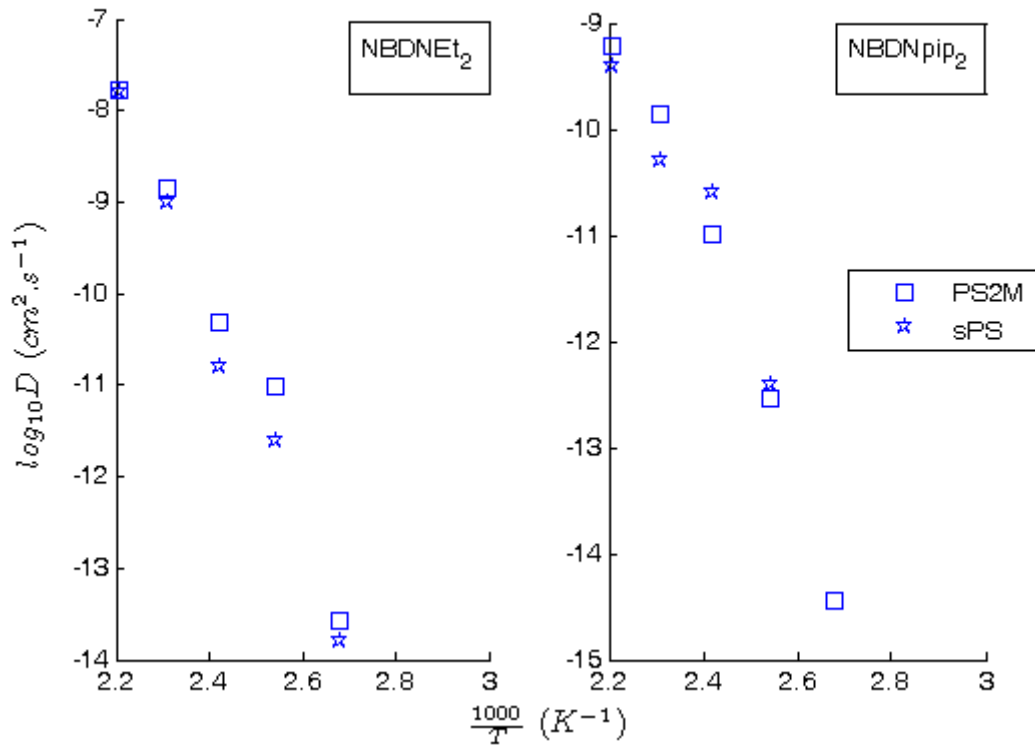


Figure 7. Comparison of the diffusion of two probes in amorphous (PS2M) or semi crystalline polystyrenes (sPS). Probes structures are given in table 2.

1
2
3
4 1 **List of abbreviations**
5
6

- 7 2 M_w Molecular weight
8 3 D diffusion coefficient (
9 4 E_a Activation energy
10 5 FRAP Fluorescence recovery after photo bleaching
11 6 A'_p tabulated polymer parameters (from the Piringer diffusion model)
12 7 C tabulated polymer parameters (from the Piringer diffusion model)
13 8 T temperature
14 9 D^* overestimated diffusion coefficient (obtained from the Piringer model)
15 10 D'_0 diffusion coefficient at infinite temperature (from the Limm model)
16 11 α tabulated polymer parameters (from the Limm model)
17 12 K tabulated polymer parameters (from the Limm model)
18 13 PVC, polyvinylchloride
19 14 PA polyamide
20 15 RH relative humidity
21 16 PET polyethylene terephthalate
22 17 PS2M Polystyrene with High molecular weight (amorphous PS)
23 18 sPS syndiotactique polystyrene (semi-crystalline)
24 19 ROI region of interest
25 20 NBD : NBD is the fluorescent kernel of the probes (nitrobenzoxadiazol)
26
27
28
29
30
31
32
33
34
35
36
37
38
39
40
41
42
43
44
45
46
47
48
49
50
51
52
53
54
55
56
57
58
59
60